

A new test of $f(R)$ gravity with the cosmological standard rulers in radio quasars

Tengpeng Xu,¹ Shuo Cao,^{1*} Jingzhao Qi,¹ Marek Biesiada,^{1,2}
Xiaogang Zheng,¹ Zong-Hong Zhu¹

¹ Department of Astronomy, Beijing Normal University, Beijing 100875, China; caoshuo@bnu.edu.cn

² Department of Astrophysics and Cosmology, Institute of Physics, University of Silesia, Uniwersytecka 4, 40-007 Katowice, Poland

Abstract. As an important candidate gravity theory alternative to dark energy, a class of $f(R)$ modified gravity, which introduces a perturbation of the Ricci scalar R in the Einstein-Hilbert action, has been extensively applied to cosmology to explain the acceleration of the universe. In this paper, we focus on the recently-released VLBI observations of the compact structure in intermediate-luminosity quasars combined with the angular-diameter-distance measurements from galaxy clusters, which consists of 145 data points performing as individual cosmological standard rulers in the redshift range $0.023 \leq z \leq 2.80$, to investigate observational constraints on two viable models in $f(R)$ theories within the Palatini formalism: $f_1(R) = R - \frac{a}{R^b}$ and $f_2(R) = R - \frac{aR}{R+ab}$. We also combine the individual standard ruler data with the observations of CMB and BAO, which provides stringent constraints. Furthermore, two model diagnostics, $Om(z)$ and statefinder, are also applied to distinguish the two $f(R)$ models and Λ CDM model. Our results show that (1) The quasars sample performs very well to place constraints on the two $f(R)$ cosmologies, which indicates its potential to act as a powerful complementary probe to other cosmological standard rulers. (2) The Λ CDM model, which corresponds to $b = 0$ in the two $f(R)$ cosmologies is still included within 1σ range. However, there still exists some possibility that Λ CDM may not be the best cosmological model preferred by the current high-redshift observations. (3) Given the current standard ruler data, the information criteria indicate that the cosmological constant model is still the best one, while the $f_1(R)$ model gets the smallest observational support. (4) The $f_2(R)$ model, which evolves quite different from $f_1(R)$ model at early times, still significantly deviates from both $f_1(R)$ and Λ CDM model at the present time.

Keywords: cosmology, cosmological parameters

Contents

1	Introduction	1
2	The $f(R)$ gravity in the metric formalism	2
3	Observational data and fitting method	5
3.1	Quasars and galaxy clusters	5
3.2	BAO and CMB data	6
4	Observational constraints	8
4.1	$f_1(R)$ model: $f_1(R) = R - \frac{a}{R^b}$	8
4.2	$f_2(R)$ model: $f_2(R) = R - \frac{aR}{R+ab}$	9
4.3	Model selection	10
5	The model diagnostics	11
5.1	$Om(z)$ diagnostic	11
5.2	Statefinder diagnostic	12
6	Conclusions and discussions	13
7	Acknowledgments	15

1 Introduction

In order to explain the accelerated expansion of the Universe, which was strongly supported by the observations of the type Ia supernovae (SN Ia) [1], a mysterious component with negative pressure was introduced as a new cosmological component dubbed as dark energy (DE). Following this this direction, based on the cosmological principles (homogeneous, isotropic) and Einstein's general relativity (GR), the current standard cosmological model considers the cosmological constant (Λ) corresponding to a modification of the energy-momentum tensor in Einstein equations, which is generally consistent with most of the observational data including SN Ia, the cosmic microwave background (CMB) [2], the baryon acoustic oscillations (BAO) [3], etc. However, considering the fact that Λ CDM is still confronted with the well-known coincidence problem and fine-tuning problem, a large number of dark energy models have been proposed to explain the cosmic acceleration [4–6]. On the other hand, without introducing the new component in the universe, the modification of general relativity provides another way to go. Some popular theories of modifying GR include $f(R)$ theory of gravity [7, 8], $f(T)$ gravity [9–11], Gauss-Bonnet and $f(G)$ gravity [12]. In this paper, we focus on the so-called $f(R)$ gravity, the advantage of which not only lies in its ability to explain the late-time cosmic acceleration of the universe, but also describe the large scale structure distribution of the Universe [13, 14]. In the framework of $f(R)$ theories of gravity, the Einstein-Hilbert Lagrangian can be modified by changing the Ricci scalar R to $f(R)$, a differentiable function of R , on the base of which the generalized field equation is derived by varying the action with respect to the metric. However, since this method always leads to fourth-order equations along with some instability problems in many interesting cases [15],

we consider in our analysis a different method called Palatini approach [7, 8], which takes the metric and the connection as two independent field variables in the action, and varies the action respectively with the two variables to obtain the generalized Einstein field equation.

From the observational point of view, it is also very important to explore such $f(R)$ cosmological models in light of observational data, which has been broadly studied in the literature [16–18]. There are two direct standard probes of expansion history of the Universe, one is the standard candles providing the information of luminosity distance ($D_L(z)$), and the other is the standard rulers related to the so-called angular diameter distance ($D_A(z)$). For instance, BAO and CMB peak locations are respectively recognized as the standard rulers [19–21], and the increasing observations of these two distance indicators have been widely used in various cosmological studies. Other most commonly used standard rulers in cosmology also include the strongly gravitationally lensed systems [22–26], the x-ray gas mass fraction of galaxy clusters [27], etc. In this paper we investigate the constraints on the $f(R)$ gravity from the latest measurement of angle diameter distance from the recently-released VLBI observations of the compact structure in intermediate-luminosity quasars [28, 29] combined with the angular-diameter-distance measurements from galaxy clusters [30], which consists of 145 data points performing as individual cosmological standard rulers in the redshift range $0.023 \leq z \leq 2.80$. Compared with other standard rulers extensively used in the literature (BAO, strong lensing systems), quasars (QSO) are observed at much higher redshifts ($z \sim 3.0$), which indicates their potential to test the $f(R)$ theory with the newly revised observations. Previous papers have demonstrated the success of this sample in its cosmological application. In Paper I [28], we demonstrated the existence of dark energy in the Universe with high significance and estimated the speed of light referring to a distant past ($z = 1.70$). In Paper II and III [29, 31], we investigated the cosmological application of this data set and obtained stringent constraints on the parameters in various dark energy models and $f(T)$ gravity models. More specifically, in this paper we try to give a new approach to constraining two viable $f(R)$ models within the Palatini formalism: $f_1(R) = R - \frac{a}{R^b}$ and $f_2(R) = R - \frac{aR}{R+ab}$, both of which can result in the radiation-dominated, matter-dominated and recent accelerating state. In order to discuss the differences between the two $f(R)$ models and Λ CDM model, we apply the information criteria (IC) [32, 33], the $Om(z)$ diagnostic [34] and the statefinder diagnostic [35] to analyse different cosmological models.

This paper is organized as follows. In Section 2, we briefly describe the basic theory of $f(R)$ gravity as well as the corresponding cosmological models. In Section 3, we describe the methodology and observational samples for angular diameter distances. In Section 4, we perform a Markov Chain Monte Carlo (MCMC) analysis, and furthermore apply model diagnostics in Section 5. Finally, the conclusions are summarized in Section 6. The units with constant speed of light $c = 1$ is used throughout this work.

2 The $f(R)$ gravity in the metric formalism

In this section we firstly derive the modified Einstein field equations in $f(R)$ theory as well as the new Friedman equation in $f(R)$ cosmology, and then briefly introduce the two $f(R)$ models in Palatini formalism to be considered in this paper.

In Palatini formalism, the modified Einstein-Hilbert action in the framework of $f(R)$ gravity is given by

$$S = \frac{1}{2\kappa} \int d^4x \sqrt{-g} f(R) + S_M(g_{\mu\nu}, \psi), \quad (2.1)$$

where $\kappa = 8\pi G$, g is the determinant of the metric $g_{\mu\nu}$, f is a differentiable function of the Ricci scalar R , and S_M is the action of matter depending on the matter field ψ and the metric $g_{\mu\nu}$. It should be noted that the metric $g_{\mu\nu}$ and the affine connection $\hat{\Gamma}_{\mu\nu}^\rho$ are treated as two independent fields for the gravity action in Palatini formalism. From the affine connection $\hat{\Gamma}_{\mu\nu}^\rho$, the expression of the generalized Ricci tensor can be written as

$$\hat{R}_{\mu\nu} = \hat{\Gamma}_{\mu\nu,\sigma}^\sigma - \hat{\Gamma}_{\mu\sigma,\nu}^\sigma + \hat{\Gamma}_{\sigma\rho}^\sigma \hat{\Gamma}_{\mu\nu}^\rho - \hat{\Gamma}_{\mu\rho}^\sigma \hat{\Gamma}_{\sigma\nu}^\rho, \quad (2.2)$$

and the Ricci scalar is dependent on the metric and the affine connection as $R = g^{\mu\nu} \hat{R}_{\mu\nu}$. Varying the action (2.1) with respect to the connection $\hat{\Gamma}$ yields the equation

$$\hat{\nabla}_\alpha [f'(R) \sqrt{-g} g^{\mu\nu}] = 0, \quad (2.3)$$

where $f'(R) \equiv df/dx$, and $\hat{\nabla}$ is the covariant derivative corresponding to the affine connection $\hat{\Gamma}$. From this equation it can be easily found that, considering a new metric $h_{\mu\nu} = f'(R)g_{\mu\nu}$ conformal with the original metric $g_{\mu\nu}$, the affine connection $\hat{\Gamma}$ can be written as the usual Levi-Civita connection of the new metric $h_{\mu\nu}$

$$\hat{\Gamma}_{\mu\nu}^\lambda = \frac{h^{\lambda\sigma}}{2} (h_{\nu\sigma,\mu} + h_{\mu\sigma,\nu} - h_{\mu\nu,\sigma}). \quad (2.4)$$

Thus we can derive the relation between the generalized affine connection $\hat{\Gamma}$ and the metric $g_{\mu\nu}$ as

$$\hat{\Gamma}_{\mu\nu}^\lambda = \Gamma_{\mu\nu}^\lambda + \frac{1}{2f'} [2\delta_{(\mu}^\lambda \partial_{\nu)} f' - g^{\lambda\tau} g_{\mu\nu} \partial_\tau f']. \quad (2.5)$$

Substituting the above equations into Eq. (2.2), the dependency between the generalized Ricci tensor $\hat{R}_{\mu\nu}$ and the original Ricci tensor $R_{\mu\nu}$ can be expressed as

$$\hat{R}_{\mu\nu} = R_{\mu\nu} - \frac{3}{2} \frac{\nabla_\mu f' \nabla_\nu f'}{f'^2} + \frac{\nabla_\mu \nabla_\nu f'}{f'} + \frac{1}{2} g_{\mu\nu} \frac{\nabla^\mu \nabla_\nu f'}{f'}. \quad (2.6)$$

From the discussion above, one can see that varying the action (2.1) with respect to the connection $\hat{\Gamma}$ gives the new geometric properties of space-time with the metric $g_{\mu\nu}$. On the other hand, by varying the action (2.1) with the metric $g_{\mu\nu}$, we can get the generalized Einstein field equation

$$f' \hat{R}_{\mu\nu} - \frac{f}{2} g_{\mu\nu} = \kappa T_{\mu\nu}, \quad (2.7)$$

where $T_{\mu\nu}$ is the energy-momentum tensor of matter. It is obvious that when $f(R) = R$, Eq. (2.7) will reduce to the Einstein field equation, while Eq. (2.7) recovers the Einstein field equation in Λ CDM model when $f(R) = R - 2\Lambda$.

Now we will introduce the $f(R)$ cosmology in the framework of flat Friedman - Robertson - Walker (FRW) metric given by

$$ds^2 = -dt^2 + a^2(t)(dx^2 + dy^2 + dz^2) \quad (2.8)$$

where $a(t)$ is the scale factor related to the redshift z as: $a(t) = (1+z)^{-1}$. Then the Hubble parameter can be expressed in terms of the scale factor: $H = \dot{a}/a$, where the overdot denotes the derivative with respect to the cosmic time t . Here we adopt the Hubble constant prior $H_0 = 69.6 \pm 0.7 \text{ kms}^{-1}\text{Mpc}^{-1}$ from the recent measurements of Hubble constant with 1%

uncertainty [36]. In the $f(R)$ cosmology, considering the cosmic fluid as a pressureless dust satisfying $p_m = 0$, we have $T_{\mu\nu} = (\rho_m + p_m)U_\mu U_\nu + p_m g_{\mu\nu} = \rho_m U_\mu U_\nu$, where U_μ , ρ_m and p_m are the 4-velocity of the fluid, the energy density and the fluid pressure, respectively. The trace of $T_{\mu\nu}$ is $T = g^{\mu\nu} T_{\mu\nu} = -\rho_m = -\rho_{m0}(1+z)^3$. Contracting Eq. (2.7) with $g^{\mu\nu}$, we can derive

$$Rf'(R) - 2f(R) = -\kappa\rho_m = -\kappa\rho_{m0}(1+z)^3. \quad (2.9)$$

Taking the time derivative of Eq. (2.9) and combining it with the conservation equation $\dot{\rho}_m + 3H\rho_m = 0$, we obtain

$$\dot{R} = \frac{3H\kappa\rho_m}{Rf'' - f'}. \quad (2.10)$$

Next we can derive the generalized Friedman equation by using the generalized Ricci tensor

$$6\left(H + \frac{1}{2}\frac{f'}{f'}\right)^2 = \frac{3f - Rf'}{f'}. \quad (2.11)$$

Substituting Eq. (2.10) into Eq. (2.11), the Friedman equation in $f(R)$ cosmology expresses as

$$H^2 = \frac{3f - Rf'}{6f'\eta^2}, \quad (2.12)$$

where

$$\eta = 1 - \frac{3f''}{2f'} \frac{Rf' - 2f}{Rf'' - f'}. \quad (2.13)$$

Correspondingly, the angular diameter distance at redshift z in flat FRW metric reads

$$\begin{aligned} D_A(z) &= \frac{1}{1+z} \int_0^z \frac{dz}{H(z)} \\ &= \frac{1}{3} (2f - Rf')^{-\frac{1}{3}} \int_{R_0}^{R_z} \frac{Rf'' - f'}{(2f - Rf')^{\frac{2}{3}}} \frac{dR}{H(R)} \end{aligned} \quad (2.14)$$

In this paper, we consider two specific viable $f(R)$ models in the Palatini approach

$$\begin{aligned} f_1(R) &= R - \frac{a}{R^b}, \\ f_2(R) &= R - \frac{a}{1 + \frac{a}{R}}. \end{aligned}$$

As the most commonly used parametrization in $f(R)$, the first model has been tested with various observational data in many previous works [37–42]. The second model is originated from the well-known Hu & Sawicki model [43], $f(R) = R - m^2 \frac{c_1(R/m^2)^n}{1+c_2(R/m^2)^n}$. Considering that n is an integer satisfying $n > 0.9$, for simplicity we have set $n = 1$ and thus $a = m^2 c_1/c_2$ and $b = 1/c_1$ in this work. In the two $f(R)$ models, one can easily find that

$$\lim_{b \rightarrow 0} f(R) = R - a, \quad (2.15)$$

which is equivalent to the Λ CDM model: $f(R) = R - 2\Lambda$, where Λ is the cosmological constant. Therefore, there are two independent model parameters (a, b) in the two $f(R)$ models, both of which can reduce to Λ CDM when $b \rightarrow 0$. We note that b can be regarded as the deviation parameter quantifying the deviation of $f(R)$ gravity from Λ CDM. Moreover, for a specific $f(R)$ model with certain value of a and b , the combination of Eq. (2.12) and (2.9) will provide the matter density parameter Ω_m , which is defined as $\Omega_m = \kappa\rho_{m0}/(3H_0^2)$. Therefore, constraint results on the $f(R)$ models can be shown in the (a, b) or (Ω_m, b) plane, which will be specifically presented in section 4.

3 Observational data and fitting method

3.1 Quasars and galaxy clusters

It has been a long-time controversy that whether compact structure in radio sources could provide a new type of standard ruler in the universe [44–47]. Recently, based on a 2.29 GHz VLBI all-sky survey of 613 milliarcsecond ultra-compact radio sources [48, 49], Cao et al. [28] presented a method to divide the full sample into different sub-samples, according to their optical counterparts and intrinsic luminosity. The final results indicated that intermediate-luminosity quasars show negligible dependence on both redshifts z and intrinsic luminosity L , and thus represent a fixed comoving-length of standard ruler. More recently, based on a cosmological-model-independent method to calibrate the linear sizes l_m of intermediate-luminosity quasars, Cao et al. [29] investigated the cosmological application of this data set and obtained stringent constraints on both the matter density parameter Ω_m and the Hubble constant H_0 , which agree well with the recent *Planck* results. The constraining power of the quasar data was also studied in viable $f(T)$ gravity models, where T is the torsion scalar in teleparallel gravity [31].

In our analysis, we will use the observations of 120 intermediate-level quasars covering the redshift range $0.46 < z < 2.80$, while the linear size of this standard ruler is calibrated to $l_m = 11.03 \pm 0.25$ pc by a new cosmological-independent technique (see Cao et al. [29] for details and reference to the source papers). The observable in this data set is the angular size of the compact structure in radio quasars, the theoretical counterpart of which expresses as

$$\theta(z) = \frac{l_m}{D_A(z)} \quad (3.1)$$

where D_A is the angular diameter distance at redshift z (Eq.(2.14)). In this work minimize the χ^2 objective function to derive model parameters of the $f(R)$ theory:

$$\chi_{\text{QSO}}^2(z; \mathbf{p}) = \sum_{i=1}^{120} \frac{[\theta_{\text{th}}(z_i; \mathbf{p}) - \theta_{\text{obs}}(z_i)]^2}{\sigma_{\theta}(z_i)^2}, \quad (3.2)$$

where \mathbf{p} represents the model parameters in $f(R)$ gravity, and $\theta_{\text{th}}(z_i; \mathbf{p})$ is the theoretical value of the angular size at redshift z_i , while $\theta_{\text{obs}}(z_i)$ and $\sigma_{\theta}(z_i)$ are the observed value and the corresponding 1σ uncertainty of angular size for each quasar, respectively. Moreover, we have considered the intrinsic spread in linear sizes l_m by adding 10% systematical uncertainty in the observed angular sizes in computing. One should note that, in the framework of χ^2 minimization method, the additional 10% uncertainties in the observed angular sizes is equivalent to adding an additional 10% uncertainty in the linear size, although the best-fit parameters describing the dependence of l_m on the luminosity and redshift are negligibly small [28, 29].

Moreover, the observations from Sunyaev-Zeldovich effect (SZE) and X-ray surface brightness from galaxy clusters also offer a source of angular diameter distances. Considering the redshift range of quasar sample used in our analysis, i.e., the lack of low-redshift quasars at $z < 0.5$, we also consider 25 galaxy clusters covering the redshift range $0.023 \leq z \leq 0.784$ from De Filippis et al. (2005) sample [50], in which a isothermal elliptical β model was used to describe the clusters by combining their SZE and X-ray surface brightness observations. As previously noted by Ref. [29], due to the the redshift coverage of high-redshift quasars and low-redshift clusters, the combination of these two astrophysical probes could contribute

a relatively complete source of angular diameter distances. The observable in this data is the angular diameter distance $D_{A,\text{obs}}$, the theoretical counterpart $D_{A,\text{th}}$ is defined in Eq. (2.14). Similar to the quasars data, the χ^2 function for the galaxy cluster data is given by

$$\chi_{\text{cluster}}^2(z; \mathbf{p}) = \sum_{i=1}^{25} \frac{[D_{A,\text{th}}(z_i; \mathbf{p}) - D_{A,\text{obs}}(z_i)]^2}{\sigma_{D_A}(z_i)^2}. \quad (3.3)$$

where σ_{D_A} is the 1σ uncertainty of the angular diameter distance for each galaxy cluster.

3.2 BAO and CMB data

Besides the individual standard rulers, observations the other two standard rulers that we shall use in this paper for the joint cosmological analysis are the BAO and CMB data.

For CMB, we use the measurement of the shift parameter \mathcal{R} , which is sensitive to the distance to the decoupling epoch corresponding to the overall amplitude of the acoustic peaks. In $f(R)$ cosmology it can be expressed as

$$\begin{aligned} \mathcal{R} &= \sqrt{\Omega_m H_0^2} \int_0^{z_*} \frac{dz}{H(z)} \\ &= 3^{-4/3} (\Omega_m H_0^2)^{1/6} \int_{R_0}^{R_*} \frac{R f'' - f'}{(2f - R f')^{2/3}} \frac{dR}{H(R)}, \end{aligned} \quad (3.4)$$

where the redshift of photon-decoupling period can be calculated as [51]

$$z_* = 1048 [1 + 0.00124 (\Omega_b h^2)^{-0.738}] [1 + g_1 (\Omega_m h^2)^{g_2}] \quad (3.5)$$

$$g_1 = \frac{0.0783 (\Omega_b h^2)^{-0.238}}{1 + 39.5 (\Omega_b h^2)^{0.763}}, \quad g_2 = \frac{0.560}{1 + 21.1 (\Omega_b h^2)^{1.81}}. \quad (3.6)$$

In this analysis, the baryon density is fixed at $\Omega_b h^2 = 0.02222$ and the shift parameter is taken as $\mathcal{R} = 1.7499 \pm 0.0088$ from the first year data release of *Planck* observations [52]. Therefore the χ^2 can be defined as

$$\chi_{\text{CMB}}^2 = \frac{(\mathcal{R} - 1.7499)^2}{0.0088^2}. \quad (3.7)$$

For BAO, we turn to the latest observations of acoustic-scale distances from the 6-degree Field Galaxy Survey (6dFGS) at lower redshift $z = 0.106$ [53], the Sloan Digital Sky Survey (SDSS-DR7) catalog combined with galaxies from 2dFGRS (at effective redshift $z = 0.2$ and $z = 0.3$) [54], while the higher- z measurement is derived from the WiggleZ galaxy survey, which reported distances in three correlated redshift bins between 0.44 and 0.73 [55]. More specifically, we use the measurement of distance ratio $\mathcal{A}(z_{\text{BAO}}) = d_A(z_*)/D_V(z_{\text{BAO}})$ from the BAO peak to set constraint on $f(R)$ model parameters, where D_V is the dilation scale and d_A is the co-moving angular diameter distance (different from the angular diameter distance D_A). The expressions of the two types of distances respectively read

$$d_A(z) = \int_0^z \frac{dz'}{H(z')} = (1+z) D_A(z) \quad (3.8)$$

$$D_V(z) = (d_A(z)^2 \frac{z}{H(z)})^{1/3}. \quad (3.9)$$

z_{BAO}	0.106	0.20	0.35	0.44	0.60	0.73
Survey	6dFGS	SDSS-DR7	SDSS-DR7	WiggleZ	WiggleZ	WiggleZ
$\frac{d_A(z_*)}{D_V(z_{BAO})}$	30.95 ± 1.46	17.55 ± 0.60	10.11 ± 0.37	8.44 ± 0.67	6.69 ± 0.33	5.45 ± 0.31

Table 1. The measurement of distance ratio $d_A(z_*)/D_V(z_{BAO})$ from the BAO observations [53–55].

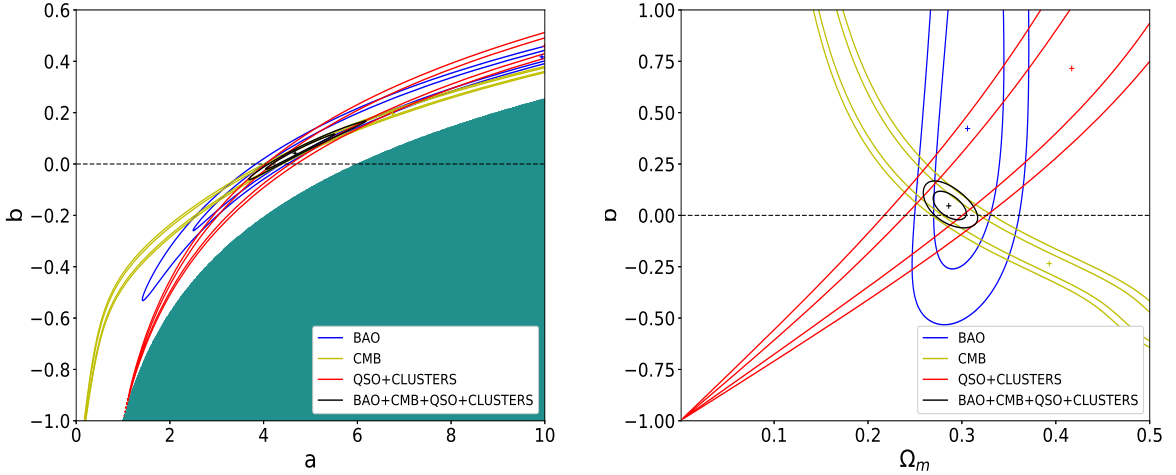


Figure 1. Confidence intervals at 68.3% and 95.4% on the (a, b) and (Ω_m, b) planes for the $f_1(R)$ model, arising from the combined fit including quasars, galaxy clusters, BAO and CMB data. The gray area represents a section of the parameter space that is not allowed, dashed line indicates the Λ CDM model with $b = 0$.

Observations of the distance ratio at six different z_{BAO} are summarized in Ref. [56] and explicitly shown in Table I. Now we can define the χ^2 for BAO as

$$\chi_{BAO}^2 = \sum_{ij} X_i C_{ij}^{-1} X_j, \quad (3.10)$$

with the difference between the theoretical and observational distance priors $X_i = \mathcal{A}_{th}(z_i) - \mathcal{A}_{obs}(z_i)$, $i = 1, 2, \dots, 6$ and the inverse covariance matrix shown in Table II [56].

C_{ij}^{-1}	1	2	3	4	5	6
1	0.48435	-0.101383	-0.164945	-0.0305703	-0.097874	-0.106738
2	-0.101383	3.2882	-2.45497	-0.0787898	-0.252254	-0.2751
3	-0.164945	-2.45497	9.55916	-0.128187	-0.410404	-0.447574
4	-0.0305703	-0.0787898	-0.128187	2.78728	-2.75632	1.16437
5	-0.097874	-0.252254	-0.410404	-2.75632	14.9245	-7.32441
6	-0.106738	-0.2751	-0.447574	1.16437	-7.32441	14.5022

Table 2. The inverse covariance matrix of the BAO observations [56].

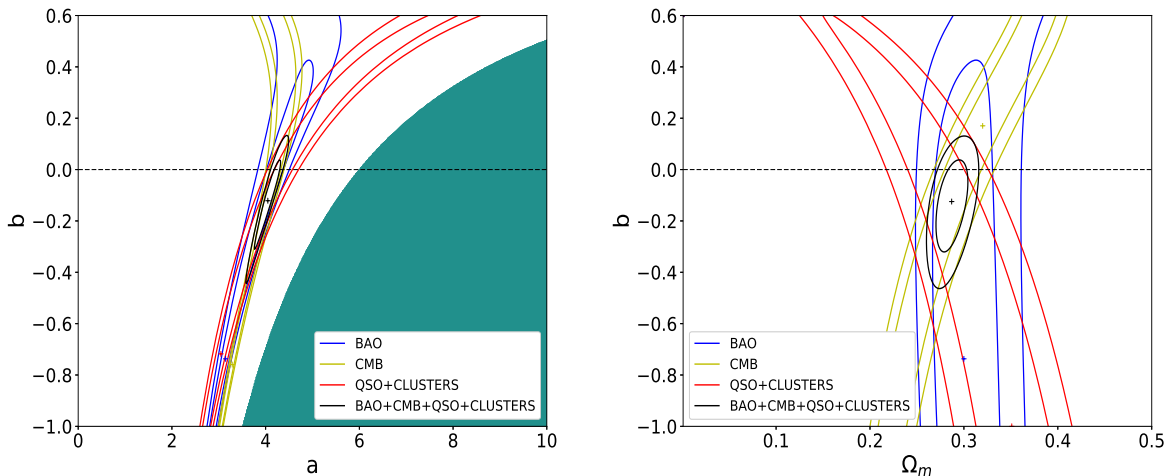


Figure 2. The same as Fig. 1, but for the $f_2(R)$ model.

4 Observational constraints

In this section, we present the constraint results of two $f(R)$ models by using different angular diameter distance data, QSO+Cluster (individual standard rulers), BAO+CMB (statistical standard rulers), and QSO+Cluster+BAO+CMB (combined standard rulers). The likelihood contours with 1σ and 2σ confidence levels for each $f(R)$ model are presented in Fig. 1 and 2, in which the left and right panels respectively illustrate the results on the (a, b) and (Ω_m, b) planes.

4.1 $f_1(R)$ model: $f_1(R) = R - \frac{a}{R^b}$

For the individual standard ruler data (QSO+Cluster), the best-fit values of the parameters in the $f_1(R)$ model are $(a, b) = (16.321, 0.715)$ or $(\Omega_m, b) = (0.417, 0.715)$. For comparison, fitting results from BAO and CMB are also shown in Fig. 1. We remark that, although the QSO+Cluster data can not tightly constrain the model parameters, the degeneracy between Ω_m and b obtained from these individual standard rulers is different from the statistical standard rulers (BAO and CMB). Therefore, the quasar data, due to the wide redshift range of $0.46 < z < 2.80$, have the potential to help break the degeneracy between model parameters in $f_1(R)$ cosmology. This tendency could also be clearly seen from the comparison between the plots obtained with BAO+CMB and the joint angular diameter distance data of QSO+Cluster+BAO+CMB. With the combined standard ruler data sets, the best-fit value for the parameters are $(a, b) = (4.669_{-0.621}^{+0.842}, 0.042_{-0.061}^{+0.074})$ or $(\Omega_m, b) = (0.286_{-0.016}^{+0.018}, 0.046_{-0.064}^{+0.068})$ within 68.3% confidence level, while the constraint results from BAO+CMB are $(a, b) = (4.349_{-1.062}^{+1.343}, 0.013_{-0.112}^{+0.116})$ or $(\Omega_m, b) = (0.296_{-0.029}^{+0.034}, 0.010_{-0.108}^{+0.116})$. Therefore, the currently compiled quasar data may significantly improve the model parameters in $f_1(R)$ cosmology.

On the other hand, the deviation parameter b from joint analysis satisfies $b = 0.046_{-0.064}^{+0.068}$ at 1σ , which indicates that Λ CDM model is still included within 68.3% confidence level. However, in the framework of exponential $f(R)$ gravity, the parameter b capturing the deviation from the concordance cosmological model seems to be slightly larger than 0, which suggests

Data	Ref.	a	b
Strong lensing	[39]	$1.50^{+12.0}_{-0.52}$	$-0.696^{+1.21}_{-0.262}$
Strong lensing+BAO+CMB	[39]	$3.75^{+2.33}_{-1.29}$	$-0.065^{+0.215}_{-0.173}$
BAO+CMB	This paper	$4.349^{+1.343}_{-1.062}$	$0.013^{+0.116}_{-0.112}$
QSO+Cluster+BAO+CMB	This paper	$4.669^{+0.842}_{-0.621}$	$0.042^{+0.074}_{-0.061}$

Table 3. Summary of the best-fit values for a and b in $f_1(R)$ model obtained from different observations.

Data	Ref.	a	b
BAO+CMB	This paper	$4.128^{+0.421}_{-0.481}$	$-0.061^{+0.350}_{-0.343}$
SNe Ia (Union 2.1)+BAO+CMB	This paper	$3.868^{+0.080}_{-0.040}$	$-0.247^{+0.119}_{-0.144}$
QSO+Cluster+BAO+CMB	This paper	$4.048^{+0.220}_{-0.281}$	$-0.121^{+0.154}_{-0.189}$

Table 4. Summary of the best-fit values for Ω_m and b in $f_2(R)$ model obtained from different observations.

that there still exists some possibility that Λ CDM may not be the best cosmological model preferred by the current observations. In order to make a good comparison with this standard Λ CDM cosmology, we fix $b = 0$ and obtain the marginalized 1σ uncertainties of model parameters as: $a = 4.389^{+0.160}_{-0.180}$, $\Omega_m = 0.270^{+0.031}_{-0.029}$ with individual standard ruler data and $a = 4.249 \pm 0.060$, $\Omega_m = 0.293 \pm 0.011$ with combined standard ruler data. In Table III we summarize the main results of this paper, which are compared with recent determinations of the parameters a and b from independent analyses of other cosmological observations.

4.2 $f_2(R)$ model: $f(R) = R - \frac{aR}{R+ab}$

Working on the $f_2(R)$ model, we find that the best fits happen at $(a, b) = (3.046, -0.718)$ or $(\Omega_m, b) = (0.340, -0.718)$ with individual standard ruler data (QSO+Cluster). By marginalizing over the parameter a , we derive the marginalized 1σ constraint on the matter density parameter $\Omega_m = 0.340$, which is well consistent with the result given by recent *Planck* first data release. The constraining power of the individual standard rulers in breaking degeneracy between model parameters is more obvious, as can be seen from the marginalized 1σ and 2σ contours of each parameter in Fig. 2. By fitting the $f_2(R)$ model to QSO+Cluster+BAO+CMB, we obtain $(a, b) = (4.048^{+0.261}_{-0.281}, -0.121^{+0.157}_{-0.189})$ or $(\Omega_m, b) = (0.287^{+0.017}_{-0.016}, -0.125^{+0.160}_{-0.196})$ at the 68.3% confidence level. Compared with the case in the $f_1(R)$ model, the largest difference happens on the constraint of b : the deviation from Λ CDM tends to be slightly smaller than 0, although the concordance cosmological scenario is still included within 68.3% confidence level. In order to compare our fits with the results obtained using the standard candles providing the information of luminosity distance, we also use the latest Union2.1 compilation consisting of 580 SN Ia data [57] to place constraint on the $f_2(R)$ model, which are specifically presented in Table IV. One can clearly see that, due to the wider redshift range of the quasars data ($0.46 < z < 2.80$) compared with SN Ia ($0.015 < z < 1.41$), the current standard ruler data make a good improvement on the constraints of the $f_2(R)$ model parameters. The recent determinations of the parameters a and b from other independent cosmological observations are also listed in Table IV.

<i>Model</i>	<i>k</i>	χ^2_{min}	<i>AIC</i>	ΔAIC	<i>BIC</i>	ΔBIC
Λ CDM	1	384.86	386.86	0	389.88	0
$f_1(R)$	2	383.87	387.87	1.01	393.92	4.04
$f_2(R)$	2	383.57	387.57	0.71	393.62	3.74

Table 5. Summary of the minimum χ^2 and the information criteria for the two $f(R)$ models, obtained from the combinations of standard rulers: CMB+BAO+QSO+Cluster. Corresponding results for the Λ CDM are also added for comparison.

4.3 Model selection

Based on a likelihood method, one may employ the information criteria (IC) to assess different models. In order to decide which $f(R)$ model is favored by the observational data, we perform model comparison statistics by using the Akaike Information Criterion (AIC) [32] and the Bayesian Information Criterion (BIC) [33]. The expressions of the two information criteria are respectively given by

$$AIC = -2\ln\mathcal{L}_{max} + 2k = \chi^2_{min} + 2k \quad (4.1)$$

and

$$BIC = -2\ln\mathcal{L}_{max} + k\ln N = \chi^2_{min} + k\ln N \quad (4.2)$$

where χ^2_{min} is the minimum χ^2 value, while k and N represent the total number of model parameters and data points. As can be clearly seen from the two information criteria, models that give a good fit with fewer parameters will be more favored by observations. The application of the BIC and AIC in a cosmological context can be found in the previous study [24, 58].

In this analysis, we use the the combined standard ruler data (quasars, galaxy clusters, BAO and CMB) for the purpose of model selection. Table V lists the value of the minimum χ^2 , AIC, BIC and the corresponding IC difference of each model ($f_1(R)$, $f_2(R)$ and Λ CDM). Note that the cosmological constant model has the lowest value of IC and the value of ΔIC is measured with respect to this model. One will find that, given the current individual standard ruler data combined with the BAO and CMB data, the information criteria indicate that the cosmological constant model is still the best one, since both the AIC and BIC values it yields are the smallest. Concerning the ranking of the two $f(R)$ models, AIC and BIC criteria give very similar conclusions, which indicate that $f_2(R)$ is slight favored, while the $f_1(R)$ model gets the smallest support from the current observations. More specifically, considering the fact that a difference in BIC (ΔBIC) of 2 is positive evidence against the model with higher BIC [33], our findings show that $f(R)$ cosmologies with more free parameters are penalized by the BIC criterion. This conclusion is in accordance with the previous results derived from other cosmological probes [24, 59].

In order to gain more insights into the above findings, in the following analysis we will turn to other sensitive and robust diagnostics to illustrate the dynamic behavior of different cosmologies. The corresponding results are obtained based on the best fits from the joint analysis of standard ruler data.

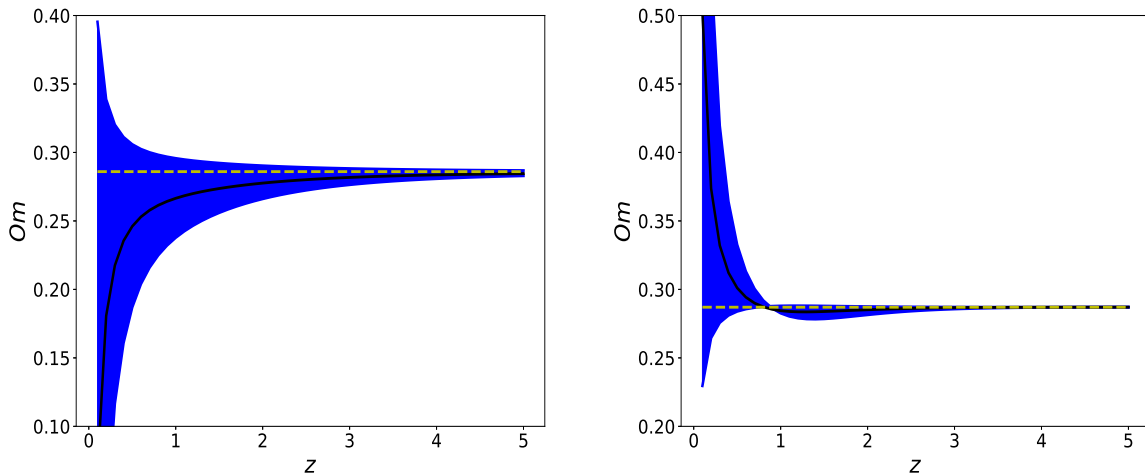


Figure 3. The evolution of $Om(z)$ versus the redshift z for $f_1(R)$ model (left panel) and $f_2(R)$ model (right panel) from the combined standard ruler data (black solid line), with the 1σ uncertainty denoted by blue shades. The standard Λ CDM model (yellow dashed line) is also added for comparison.

5 The model diagnostics

In the framework of a specific cosmological model, the Hubble parameter H and the deceleration parameter q respectively express as

$$H = \frac{\dot{a}}{a}, q = -\frac{\ddot{a}}{aH^2} = -\frac{a\ddot{a}}{\dot{a}^2}, \quad (5.1)$$

where a is the scale factor. These quantities were first propose to test both the evolution of cosmology (i.e., the determination of transition redshift (deceleration/acceleration), which has been proved to provide an efficient way for constraining cosmological models [60]), and then extensively applied to the investigation of the dynamical properties of dark energy (i.e., the possible interaction between cosmic dark sectors [61, 62]). In this section, we will perform two diagnostics analysis based on the above two quantities, i.e., the $Om(z)$ diagnostic and the statefinder diagnostic, to discuss the possibility of discriminating the three cosmological models ($f_1(R)$, $f_2(R)$ and Λ CDM).

5.1 $Om(z)$ diagnostic

The expansion rates at different redshifts, or the Hubble parameters $H(z)$, opened a new chapter in using the so called $Om(z)$ diagnostics to discriminate different cosmological models as well as Λ CDM model [34]. In this method, a new diagnostics is defined as

$$Om(z) = \frac{E^2(z) - 1}{(1+z)^3 - 1} \quad (5.2)$$

where $E(z) = H(z)/H_0$ is the dimensionless expansion rate. Neglecting the radiation component at low redshift, the Friedmann equation in the Λ CDM model is $H(z)^2 = H_0^2[\Omega_m(1+z)^3 + 1 - \Omega_m]$ and the $Om(z)$ parameter should be equal exactly to the present value of matter density $Om(z) = \Omega_m$, if the cosmological model of our universe is exactly the

Λ CDM model. Therefore, such diagnostic can be used as a cosmological probe to directly illustrate the difference between Λ CDM and other cosmological models.

Fig. 3 shows the $Om(z)$ parameter as a function of redshift for the two $f(R)$ models, with the best-fitted value as well as the 1σ uncertainties derived from the combined standard ruler data. It is obvious that the $Om(z)$ curves of the two $f(R)$ models will coincide with Λ CDM at high redshifts ($z > 3$), which indicates that the $Om(z)$ for the $f(R)$ models cannot be distinguished Λ CDM at early universe. The $f(R)$ cosmology begins to deviate from the Λ CDM at the redshift interval of $1.5 < z < 3$, although we still cannot distinguish the two $f(R)$ models at this epoch. At redshifts $z < 1$, the two $f(R)$ models begin to deviate with each other: for $f_1(R)$ model, the value of $Om(z)$ is always smaller than that in Λ CDM model, while the deviation between $f_1(R)$ and Λ CDM gradually increase, which implies a smaller $Om(z)$ in the future; for $f_2(R)$ model, the other cosmological candidate proposed without introducing dark energy in the Universe, the value of $Om(z)$ is also smaller than Ω_m when the deviation from Λ CDM model takes place, which will increase and exceed Ω_m at lower redshifts.

5.2 Statefinder diagnostic

As can be clearly seen from Eq. (5.1), the Hubble parameter H and the deceleration parameter q are respectively related to \dot{a} and \ddot{a} . Considering that H and q cannot effectively differentiate between different cosmological models, a joint analysis still requires a new parameter related to the higher order of time derivatives of a . In the so-called statefinder diagnostic [35], the statefinder pair $\{r, s\}$ is defined as

$$r = \frac{\ddot{a}}{aH^3}, \quad s = \frac{r - 1}{3(q - 1/2)} \quad (5.3)$$

where the deceleration parameter can be derived from Eq. (5.1) as

$$q(z) = \frac{E'(z)}{E(z)}(1 + z) - 1. \quad (5.4)$$

where $E'(z) \equiv dE(z)/dz$. Then the statefinder pair $\{r, s\}$ can be expressed as

$$\begin{aligned} r(z) &= 1 - 2\frac{E'(z)}{E(z)}(1 + z) + \left[\frac{E''(z)}{E(z)} + \left(\frac{E'(z)}{E(z)} \right)^2 \right] (1 + z)^2 \\ &= q(z)(1 + 2q(z)) + q'(z)(1 + z) \end{aligned} \quad (5.5)$$

$$s(z) = \frac{r(z) - 1}{3(q(z) - 1/2)} \quad (5.6)$$

where $q'(z) \equiv dq(z)/dz$. Applying the best-fitted value as well as the 1σ uncertainties derived from the combined standard ruler data for each $f(R)$ model, we figure out the evolution of statefinder pair (r, s) and the deceleration parameter q , and show the trajectories of the two $f(R)$ models in the $r - s$ and $r - q$ plane in Fig. 4 and 5. It is worth mentioning that, the statefinder parameters r and s for Λ CDM model are constants, $(r, s) = (1, 0)$ [63].

The evolution trajectories in the $r - q$ plane for different cosmological models are shown in Fig. 4. One may note that the deceleration parameter q evolves similarly for the two $f(R)$ models and Λ CDM model, while the statefinder parameter r exhibits obvious fluctuation, which indicates that the parameter r is more suitable to discriminate different cosmological

models. As can be clearly seen from Fig. 4, the curve of each cosmological model originates from the same point $(r, q) = (1, 0.5)$, evolves along different trajectory, and finally converges on the same point $(r, q) = (1, -1)$. For $f_1(R)$, the deviation from Λ CDM is not as obvious as that between $f_2(R)$ and Λ CDM, while the trajectory of $f_1(R)$ converges with Λ CDM earlier than $f_2(R)$. At the present epoch, the parameters (r, q) for $f_1(R)$ and Λ CDM cannot be distinguished from each other, while the value of r for $f_2(R)$ is larger than that of the other two models. More interestingly, it is noteworthy that for $f_2(R)$ cosmology, we observe the signature flip from negative to positive in the value of r in the early universe, which indicates that the $f_2(R)$ model is quite different from $f_1(R)$ model and Λ CDM model at early times.

The evolution of statefinder pair (r, s) for different cosmological models are plotted in Fig. 5, in which the yellow square at $(r, s) = (0, 1)$ indicates the statefinder of Λ CDM model. It is apparent that the statefinder pair of $f_2(R)$ evolves quite different from that in the framework of $f_1(R)$ CDM model. More importantly, as is shown in Fig. 5, the current value of (r, q) for $f_1(R)$ is well consistent with Λ CDM, while the corresponding value for $f_2(R)$ significantly deviates from both of them at the present epoch. Therefore, although the statefinder pair (r, q) cannot distinguish $f_1(R)$ model and Λ CDM model from each other at the present time, it is able to distinguish the $f_2(R)$ from both f_1 CDM and Λ CDM. However, the $f(R)$ cosmologies are not distinguishable and can not be distinguished from Λ CDM in the near future.

As a final comment, one should note that the combination of standard ruler data implies that, the two modified gravity models discussed in this analysis are still practically indistinguishable from Λ CDM. Such a tendency is more obvious when the 1σ uncertainty of the model parameters is taken into consideration (See Figs. 3-5). Therefore, the above conclusions still need to be checked by future high-precision VLBI observations of the compact structure in radio quasars [64, 65], which also highlights the importance of different cosmological standard rulers to provide additional observational fits on alternative candidate gravity theories.

6 Conclusions and discussions

As an important candidate gravity theory alternative to dark energy, a class of $f(R)$ modified gravity, which introduces a perturbation of the Ricci scalar R in the Einstein-Hilbert action, has been extensively applied to cosmology to explain the acceleration of the universe. On the other hand, recent observations of various cosmological standard rulers acting as distance indicators in the Universe, have provided a lot of information concerning angular diameter distance D_A . In this paper, we focused on the recently-released VLBI observations of the compact structure in intermediate-luminosity quasars combined with the angular-diameter-distance measurements from galaxy clusters, which consists of 145 data points performing as individual cosmological standard rulers in the redshift range $0.023 \leq z \leq 2.80$, to investigate observational constraints on two viable models in $f(R)$ theories within the Palatini formalism: $f_1(R) = R - \frac{a}{R^b}$ and $f_2(R) = R - \frac{aR}{R+ab}$. Here we summarize our main conclusions in more detail.

- In the framework of $f(R)$ gravity in Palatini approach, although the QSO+Cluster data can not tightly constrain the model parameters, the degeneracy between Ω_m and b obtained from these individual standard rulers is different from the statistical standard rulers (BAO+CMB). Therefore, the quasar data have the potential to help break the

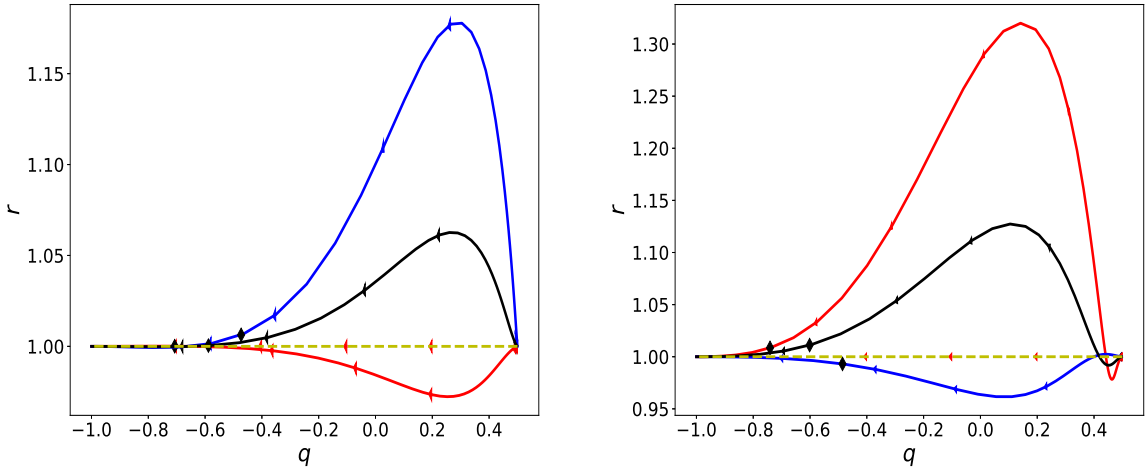


Figure 4. The evolution of (r, q) for $f_1(R)$ model and $f_2(R)$ model (black line), with the 1σ uncertainty denoted by red and blue lines. The standard Λ CDM model (yellow dashed line) is also added for comparison. The diamond point and the arrows on each curve respectively denote the current value and the evolution direction of (r, q) for each cosmological model.

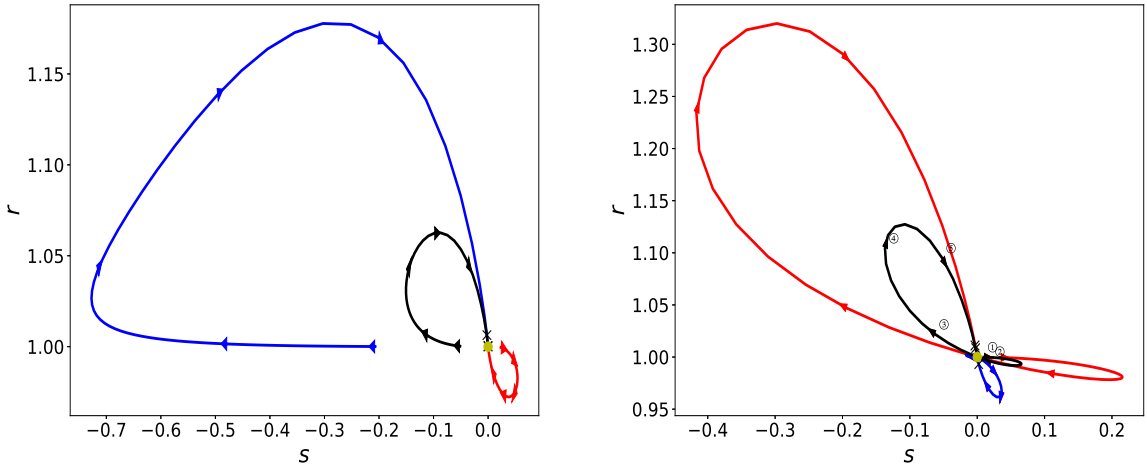


Figure 5. The same as Fig. 4, but for the evolution of (r, s) . The black cross and the arrows on each curve respectively denote the current value and the evolution direction of (r, s) for each cosmological model. The yellow square at $(r, s) = (1, 0)$ represents Λ CDM model. For $f_2(R)$, in order to represent the evolution trajectory more clearly, the circled sequence numbers are marked on the curve.

degeneracy between model parameters in $f(R)$ cosmology. More specifically, one can clearly see that, due to the wider redshift range of the quasars data ($0.46 < z < 2.80$) compared with SN Ia ($0.015 < z < 1.41$), the current standard ruler data make a good improvement on the constraints of the $f_2(R)$ model parameters.

- From the joint analysis of combined standard ruler data, the matter density parameter

Ω_m derived from the combined standard ruler data in the $f_1(R)$ and $f_2(R)$ model are both close to 0.30, which is consistent with that from other independent cosmological observations. Moreover, with the assumption of a flat universe and given the current quality of the observational data, the Λ CDM model is still included within 68.3% confidence level and there is no reason to prefer any more complex model. Given the current individual standard ruler data combined with the BAO and CMB data, the information criteria imply that the cosmological constant model is still the best one, while the $f_1(R)$ model gets the smallest support from the current observations.

- Deviation from Λ CDM cosmology is also detected in the obtained confidence level in our analysis. More specifically, in the framework of exponential $f_1(R)$ gravity, the deviation parameter b denoting the difference between $f(R)$ gravity and the concordance Λ CDM model seems to be slightly larger than 0, while for $f_2(R)$ gravity, the largest difference happens on the constraint of b , i.e., the deviation from Λ CDM tends to be slightly smaller than 0. Therefore, there still exists some possibility that Λ CDM may not be the best cosmological model preferred by the current observations. However, this conclusion still needs to be checked and confirmed by future more accurate observational data.
- Applying the best-fits from combined standard ruler data to two model diagnostics, $Om(z)$ and statefinder, we have applied two model diagnostics to differentiate the dynamical behavior of the $f(R)$ models. The results from the $Om(z)$ diagnostic show that the $Om(z)$ for the $f(R)$ models cannot be distinguished from Λ CDM at early universe. As the redshift decreases, the $f(R)$ cosmology begins to deviate from the Λ CDM at the redshift interval of $1.5 < z < 3$. On the other hand, the statefinder diagnostic indicates that in the early universe $f_2(R)$ evolves quite differently from that in the framework of $f_1(R)$ model, both of which will finally evolve to the same state. At the present time, $f_1(R)$ model is well consistent with Λ CDM model, while $f_2(R)$ model still significantly deviates from both $f_1(R)$ and Λ CDM model. However, when the 1σ uncertainty of the model parameters is taken into consideration, these two modified gravity models are still practically indistinguishable from Λ CDM.
- Given the redshift coverage of high-redshift quasars and low-redshift clusters, the combination of these two astrophysical probes could provide a relatively complete source of angular diameter distances. From the perspective of observations, the recently released quasar data propose a new way to probe the cosmology. Furthermore, the quasar data used in this paper were observed at single frequency, we expect the future high-precision observations derived at multi frequencies [64, 65] to provide more information of other classes of modified gravity theories. From the theoretical point of view, besides the two $f(R)$ models which we have already extensively investigated in this paper, some other typical examples are Lorentz violating theories [66], ghost condensation [67], and tensor-vector-scalar theory of gravity [68].

7 Acknowledgments

This work was supported by National Key R&D Program of China No. 2017YFA0402600, the National Basic Science Program (Project 973) of China under (Grant No. 2014CB845800), the National Natural Science Foundation of China under Grants Nos. 11503001, 11633001 and 11373014, the Strategic Priority Research Program of the Chinese Academy of Sciences,

Grant No. XDB23000000, the Interdiscipline Research Funds of Beijing Normal University, and the Opening Project of Key Laboratory of Computational Astrophysics, National Astronomical Observatories, Chinese Academy of Sciences. J.-Z. Qi was supported by China Postdoctoral Science Foundation under Grant No. 2017M620661. M. Biesiada was supported by Foreign Talent Introducing Project and Special Fund Support of Foreign Knowledge Introducing Project in China.

References

- [1] Riess, A. G., et al. 1998, *The Astronomical Journal*, 116, 1009
- [2] Spergel, D. N., et al. 2007, *The Astrophysical Journal Supplements*, 170, 377
- [3] Percival, W. J., et al. 2007, *Monthly Notices of the Royal Astronomical Society*, 381, 1053
- [4] Bento, M. C., et al. 2002, *Physical Review D*, 66, 043507
- [5] Xu, C., et al. 2012, *Journal of Cosmology and Astroparticle Physics*, 7, 005
- [6] Wu, P. & Yu, H. 2011, *European Physical Journal C*, 71, 1552
- [7] De Felice, A. & Tsujikawa, S. 2010, *Living Reviews in Relativity*, 13, 3
- [8] Sotiriou, T. P. & Faraoni, V. 2010, *Reviews of Modern Physics*, 82, 451
- [9] Bengochea, G. R. & Ferraro, R. 2009, *PRD*, 79, 124019
- [10] Cai, Y.-F., et al. 2015, arXiv:1511.07586
- [11] Qi, J.-Z., et al. 2016, *Research in Astronomy and Astrophysics*, 16, 002
- [12] Nojiri, S. & Odintsov, S. D. 2005, *PLB*, 631, 1
- [13] dos Santos, M. V., et al. 2016, *A&A*, 587, A132
- [14] Voivodic, R., et al. 2017, *PRD*, 95, 024018
- [15] Dolgov, A. D., & Kawasaki, M. 2003, *Physics Letters B*, 573, 1
- [16] Carvalho, F. C., Santos, E. M., Alcaniz, J. S., & Santos, J. 2008, *Journal of Cosmology and Astroparticle Physics*, 9, 008
- [17] de la Cruz-Dombriz, Á., Dunsby, P. K. S., Kandhai, S., & Sáez-Gómez, D. 2016, *Physical Review D*, 93, 084016
- [18] Song, Y.-S., Peiris, H., & Hu, W. 2007, *Physical Review D*, 76, 063517
- [19] Percival, W. J., Reid, B. A., Eisenstein, D. J., et al. 2010, *Monthly Notices of the Royal Astronomical Society*, 401, 2148
- [20] Blake, C., Kazin, E. A., Beutler, F., et al. 2011, *Monthly Notices of the Royal Astronomical Society*, 418, 1707
- [21] Beutler, F., Blake, C., Colless, M., et al. 2011, *Monthly Notices of the Royal Astronomical Society*, 416, 3017
- [22] Biesiada, M., Malec, B., & Piórkowska, A. 2011, *Research in Astronomy and Astrophysics*, 11, 641
- [23] Cao, S., & Zhu, Z.-H. 2012, *Astronomy and Astrophysics*, 538, A43
- [24] Cao, S., Covone, G., & Zhu, Z.-H. 2012, *The Astrophysical Journal*, 755, 31
- [25] Cao, S., Pan, Y., Biesiada, M., Godłowski, W., & Zhu, Z.-H. 2012, *Journal of Cosmology and Astroparticle Physics*, 3, 016

- [26] Cao, S., Biesiada, M., Gavazzi, R., Piórkowska, A., & Zhu, Z.-H. 2015, *The Astrophysical Journal*, 806, 185
- [27] Cao, S., & Zhu, Z.-H. 2014, *Physical Review D*, 90, 083006
- [28] Cao, S., Biesiada, M., Jackson, J., et al. 2017, *Journal of Cosmology and Astroparticle Physics*, 2, 012
- [29] Cao, S., Zheng, X., Biesiada, M., et al. 2017, *Astronomy and Astrophysics*, 606, A15
- [30] Bonamente, M., Joy, M. K., LaRoque, S. J., et al. 2006, *The Astrophysical Journal*, 647, 25
- [31] Qi, J.-Z., Cao, S., Biesiada, M., Zheng, X., & Zhu, Z.-H. 2017, *European Physical Journal C*, 77, 502
- [32] Akaike, H. 1974, *IEEE Transactions on Automatic Control*, 19, 716
- [33] Schwarz, G. 1978, *Annals of Statistics*, 6, 461
- [34] Sahni, V., Shafieloo, A., & Starobinsky, A. A. 2008, *Physical Review D*, 78, 103502
- [35] Pasqua, A., Chattopadhyay, S., Momeni, D., et al. 2017, *Journal of Cosmology and Astroparticle Physics*, 4, 015
- [36] Bennett, C. L., Larson, D., Weiland, J. L., & Hinshaw, G. 2014, *The Astrophysical Journal*, 794, 135
- [37] Amarzguioui, M., Elgarøy, Ø., Mota, D. F., & Multamäki, T. 2006, *Astronomy and Astrophysics*, 454, 707
- [38] Carvalho, F. C., Santos, E. M., Alcaniz, J. S., & Santos, J. 2008, *Journal of Cosmology and Astroparticle Physics*, 9, 008
- [39] Liao, K., & Zhu, Z.-H. 2012, *Physics Letters B*, 714, 1
- [40] Santos, J., Alcaniz, J. S., Carvalho, F. C., & Pires, N. 2008, *Physics Letters B*, 669, 14
- [41] Fay, S., Tavakol, R., & Tsujikawa, S. 2007, *Physical Review D*, 75, 063509
- [42] Koivisto, T. 2007, *Physical Review D*, 76, 043527
- [43] Basilakos, S., Nesseris, S., & Perivolaropoulos, L. 2013, *Physical Review D*, 87, 123529
- [44] Jackson, J. C., & Dodgson, M. 1997, *Monthly Notices of the Royal Astronomical Society*, 285, 806
- [45] Vishwakarma, R. G. 2001, *Classical and Quantum Gravity*, 18, 1159
- [46] Lima, J. A. S., & Alcaniz, J. S. 2002, *The Astrophysical Journal Supplement Series*, 566, 15
- [47] Cao, S., Biesiada, M., Zheng, X., & Zhu, Z.-H. 2015, *The Astrophysical Journal*, 806, 66
- [48] Kellermann, K. I. 1993, *Nature*, 361, 134
- [49] Gurvits, L. I. 1994, *The Astrophysical Journal*, 425, 442
- [50] Holanda, R. F. L., Lima, J. A. S., & Ribeiro, M. B. 2011, *Astronomy and Astrophysics*, 528, L14
- [51] Hu, W., & Sugiyama, N. 1996, *The Astrophysical Journal*, 471, 542
- [52] Planck Collaboration, Ade, P. A. R., Aghanim, N., et al. 2014, *Astronomy and Astrophysics*, 571, A16
- [53] Beutler, F., Blake, C., Colless, M., et al. 2011, *Monthly Notices of the Royal Astronomical Society*, 416, 3017
- [54] Percival, W. J., Reid, B. A., Eisenstein, D. J., et al. 2010, *Monthly Notices of the Royal Astronomical Society*, 401, 2148

- [55] Blake, C., Brough, S., Colless, M., et al. 2012, *Monthly Notices of the Royal Astronomical Society*, 425, 405
- [56] Giostri, R., Vargas dos Santos, M., Waga, I., et al. 2012, *Journal of Cosmology and Astroparticle Physics*, 3, 027
- [57] Suzuki, N., Rubin, D., Lidman, C., et al. 2012, *The Astrophysical Journal*, 746, 85
- [58] Pan, Y., Cao, S., & Li, L. 2016, *International Journal of Modern Physics D*, 25, 1650003
- [59] Zheng, X., Biesiada, M., Cao, S., Qi, J., & Zhu, Z.-H. 2017, *Journal of Cosmology and Astroparticle Physics*, 10, 030
- [60] Chen, Y., Zhu, Z.-H., Alcaniz, J. S., & Gong, Y. 2010, *The Astrophysical Journal*, 711, 439
- [61] Cao, S., Liang, N., & Zhu, Z.-H. 2011, *Monthly Notices of the Royal Astronomical Society*, 416, 1099
- [62] Cao, S., & Liang, N. 2011, *International Journal of Modern Physics D*, 22, 1350082
- [63] Huang, Z. G., Song, X. M., Lu, H. Q., & Fang, W. 2008, *Astrophysics and Space Science*, 315, 175
- [64] Pushkarev, A. B., & Kovalev, Y. Y. 2015, *MNRAS*, 452, 4274
- [65] Cao, S., Biesiada, M., Zheng, X., et al. 2017, arXiv:1708.08639
- [66] Libanov, M., Rubakov, V., Papantonopoulos, E., Sami, M., & Tsujikawa, S. 2007, *Journal of Cosmology and Astroparticle Physics*, 8, 010
- [67] Hamed, N. A., Cheng, H. S., Luty, M. A., & Mukohyama, S. 2004, *Journal of High Energy Physics*, 5, 074
- [68] Bekenstein, J. D. 2005, *Physical Review D*, 71, 069901